Photogrammetry - Selected Chapters (PSC)
2019 WS

River monitoring using Aerial Images

Himanshi Singhal

ESPACE - Earth oriented space science and technology

Table of Content

Why River Monitoring?

82% of world's population live on previously flooded land (Diley et al. 2005) & 87% have rivers as their closest water body (Kummu et. al. 2011)

- Environmental, economic & societal role – food, water, nutrients, transport, potential energy, supporting biodiversity & freshwater resources etc.
- World's most dangerous natural hazards – banks erosion, flooding & droughts

Why River Monitoring?

Monitor river quantity and quality (water health)

- River characterization – River discharge, aquatic ecology (mapping species coverage and their distribution), banks erosion, sedimentary transfer process by identifying and assessing dry, wet, shallow, deep areas etc.
- River restoration & management – Identifying the deadly algae species and other harmful constituents

Why Aerial Imagery?

- Higher spatial and temporal resolution
- Cloud free acquisitions
- Easy setup and low operational costs
- Continuous information as opposed to point based survey technique
- Mobility - Access to rural streams & areas inaccessible or dangerous or under hazardous situations

1.2 River Corridor Introduction

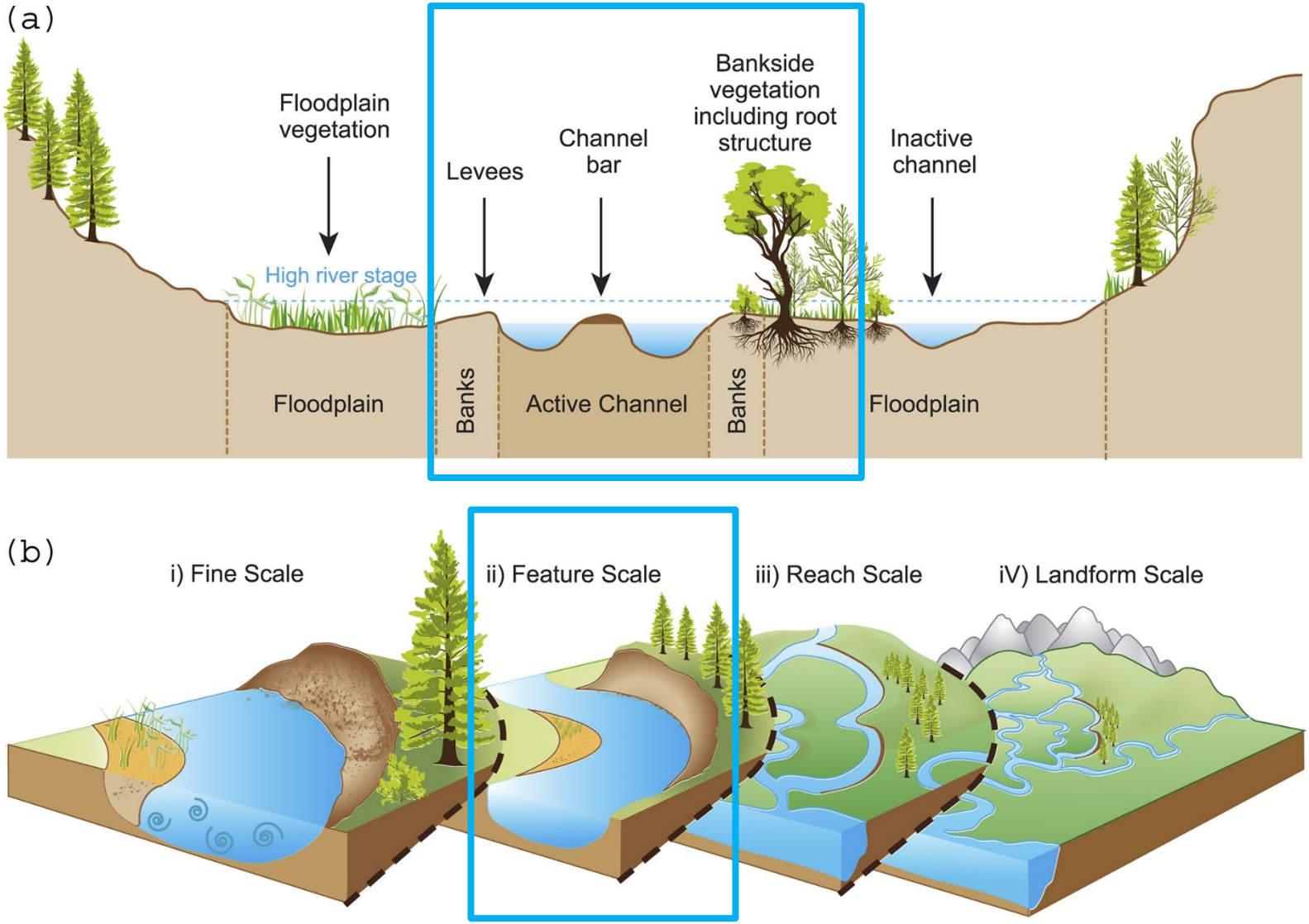

[Tomsett & Leyland (2019)]

1.3 Challenges

- Detecting the riverlines – irregular boundaries
- Occlusion by trees along the riverlines
- Vegetation shadowing in the river
- Depth of the riverbed – visibility of the bed
- Highly dynamic fluvial environment
  - Detecting and classifying the biomass
  - Detecting and classifying the sediments underneath – overlap!
- Ground Control Points Deployment for validation

1.4 Assumptions

- Photogrammetry & flight principles – consistency in imagery during the aerial flight days
  - Exposure
  - Time
  - Aperture Lighting (sunlight)
  - Wind conditions
- No obstruction along the flight path
  - No trees
  - No riffles
  - No emerging banks
- Same spectral homogenous distribution of the river throughout its corridor
- River bed is visible in the images – low depth and low turbidity

2 Overview – Solution Strategy

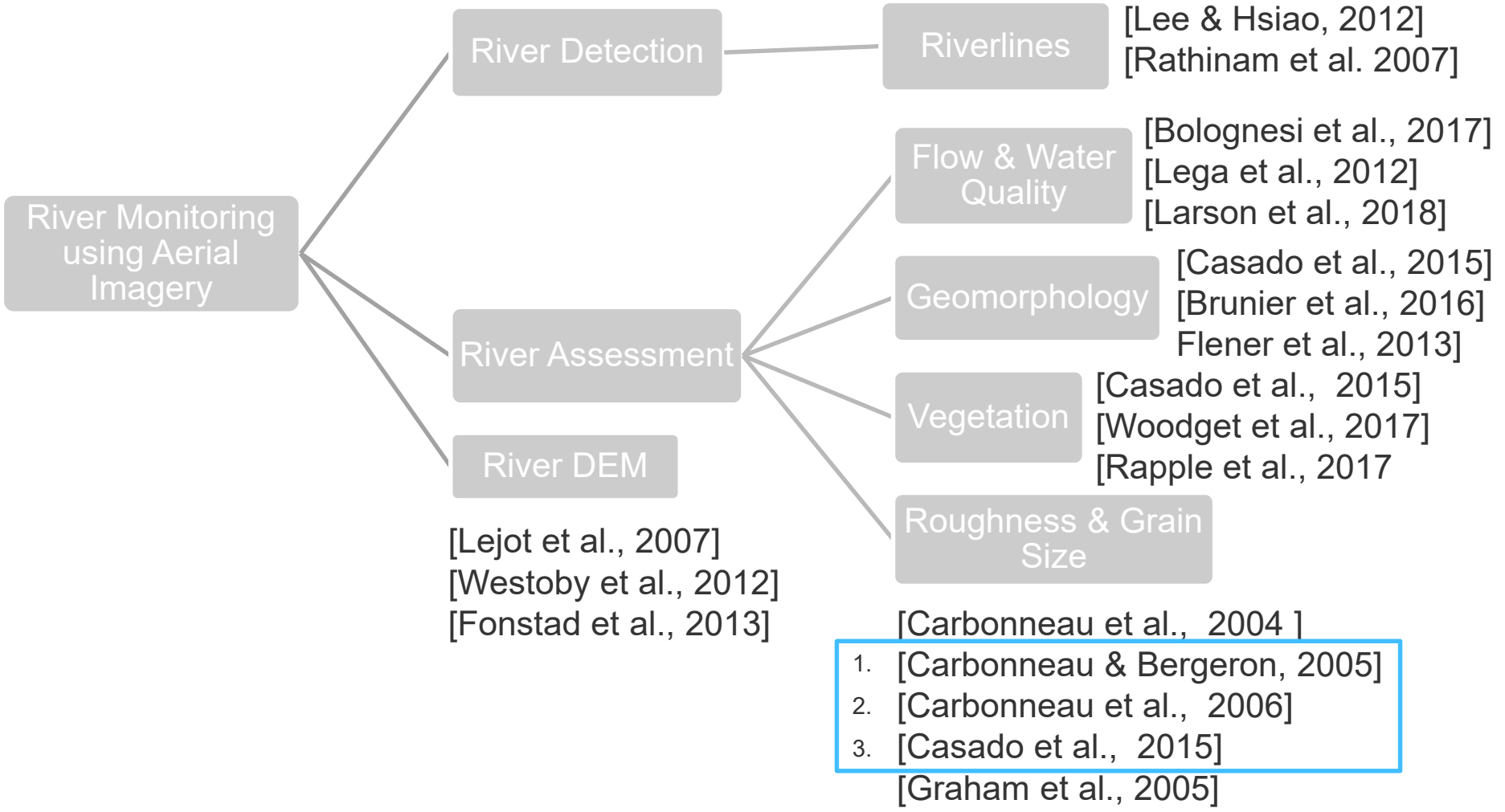

Methods

Method 1

Automated grain size measurements for long river profiles

Carbonneau P E, Bergeron N, Lane S N (2005)

Goal: Automated gravel size measurements in both dry & shallow wetted areas for long river lengths to understand sedimentary transfer process by mapping grain size variability along the river channel

- Using image processing and classification algorithms in MATLAB

- Previous approach
  - Automated grain size measurements (Carbonneau et al., 2004)
    - Limitation: Applicable only for dry areas

- Proposed approach
  - Extension of previous work to wet areas as well

- Principle
  - Delineate the individual particles using image processing techniques

$$D = a * SV + b$$

D is the median diameter (~mm) of surface particles, SV is dimensionless local semivariance, a & b constants are found by calibration

Semivariograms (1) [ArcGIS Pro]

- Depicts the spatial autocorrelation of the measured sample points
  - Semivariance - variance in brightness levels in pixels separated by a distance are a function of distance
- Fitting the data yields a model
- Three interesting parameters
  - Range – x value when the y value stops increasing
  - Sill – y value at maximum x range
  - Nugget – Initial y intercept when x is 0
- Range – points within range are correlated, outside are not
- Nugget effects happen due to measurement errors or spatial sources of variation
- Example: Checkerboard

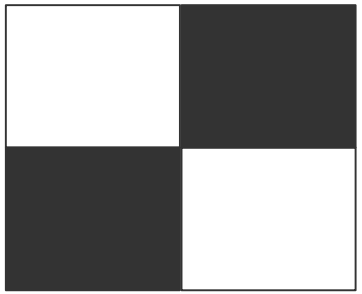

Semivariograms (2)

- Positive Autocorrelation (similar values next to each other)
  - Clusters

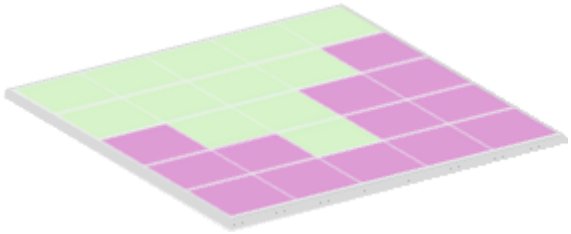

[GIS Geography]

- Negative Autocorrelation (dissimilar values next to each other)

[GIS Geography]

- For points compared to increasingly distant points - the semivariance increases, for closer points, its smaller in value

Semivariograms (3)

- Semivariograms in Grain size estimation
  - Spatial autocorrelation of the measured brightness points
    - Brightness of gravels in images
  - Assumptions
    - Gravels have light surface and dark boundaries, therefore difference in brightness of surface vs boundaries
    - Gravels are of smilar size in the area of prediction as of model calibration
    - Each gravel is covered in multiple pixels, and not, multiple gravels in pixels
      - This is to avoid the averaging effect
  - Example semivariogram
    - Sill (y value) tells the grain size

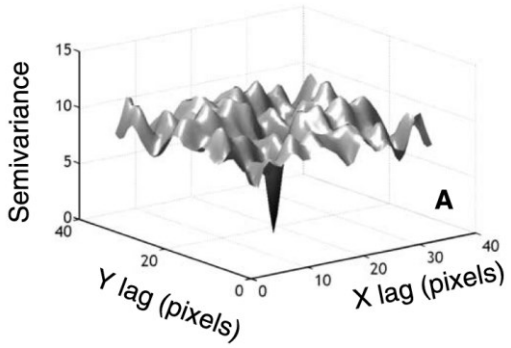

  - Fit a model to find the slope and intercept

3.1 Method 1 - Approach (1) [Carbonneau et al., 2004]

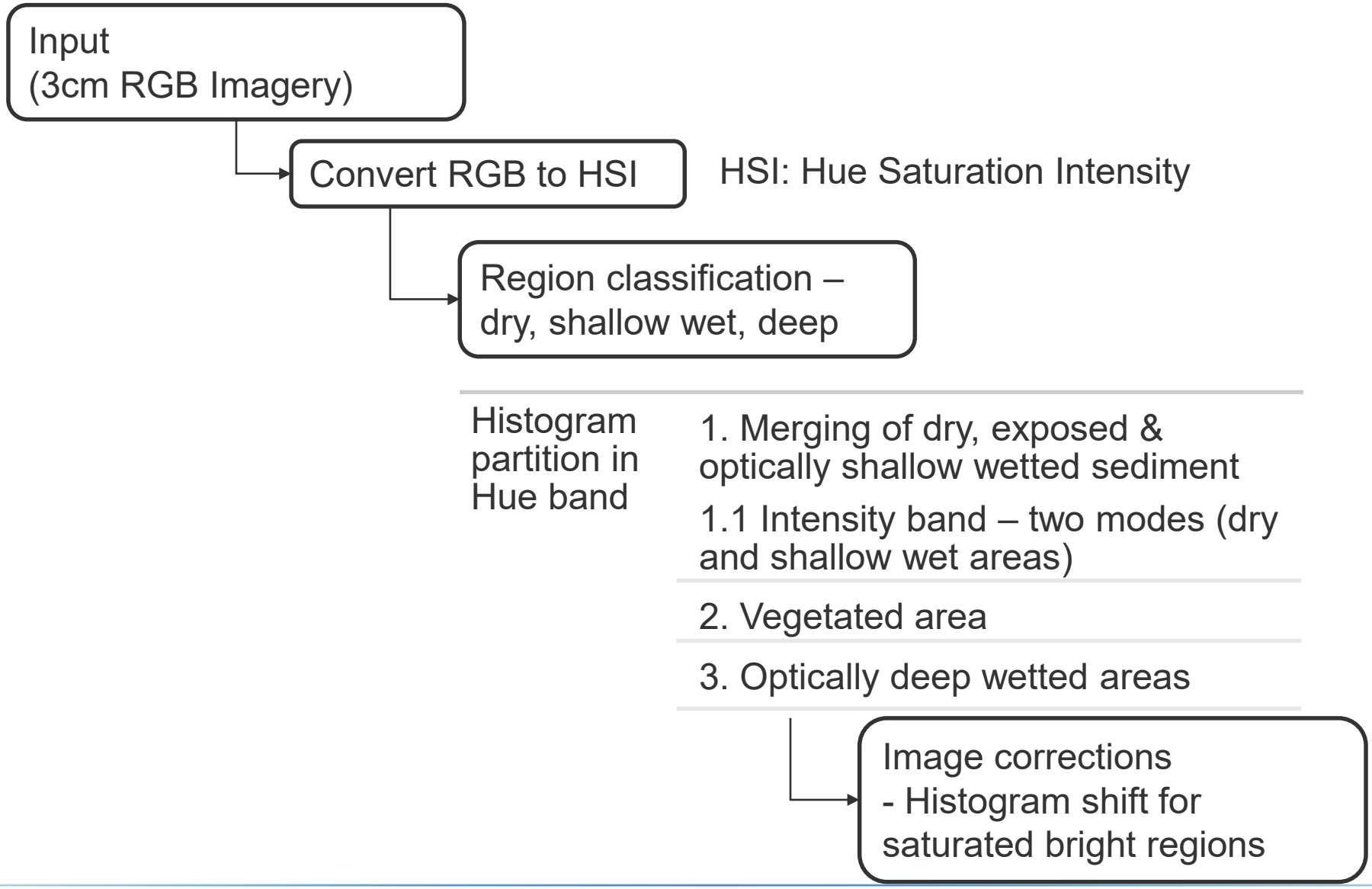

3.1 Method 1 - Approach (2) [Carbonneau et al., 2004]

Mapping Image Property – correlation between local image poperties & grain size in images

Optimal window size selection

Model calibration with ground truth – a and b constants for equation

Calibration & Validation Results

Table 1. Complete Results of Model Calibration Attempts[a]

Window Size, pixels	Pixel Size, cm	Actual Window Size, cm	Method	Slope	Intercept	R^2
5 × 5	3	15 × 15	SV	NS	NS	NS
10 × 10	3	30 × 30	SV	NS	NS	NS
20 × 20	3	60 × 60	SV	NS	NS	NS
33 × 33	**3**	**99 × 99**	**SV**	**0.34**	**10.12**	**0.80**
50 × 50	**3**	**150 × 150**	**SV**	**0.29**	**12.40**	**0.72**

3.1 Method 1 – Approach (3) [Carbonneau et al., 2005]

- Extension of Semivariance mapping to wet areas
  - Equation for dry area needs to be recalibrated for wet areas
  - Averaging window needs to be reconsidered based on the grain size
  - For dry-wet interface (each meter length)
    - Calibration : 216 points from the combination of adjacent 1m^2 of dry area and 1m^2 of wet area
- Calculate Mean brightness values for each image
- Assign zero pixels as the mean pixel values to minimize the edge contrast between the masked area and class-imaged area
- Semivariance mapping on images by windowed semivariogram equation
- Conversion of semivariance maps to grain size maps

Dry areas: $D_{50} = 0.34SV + 10.12 \longrightarrow$ Wet areas: $D_{50} = 1.33SV + 18.95$

Method 2

Estimate depth-color relationship using illumination corrections

Carbonneau P E, Lane S N, Bergeron N (2006)

Goal: Improve prediction quality using illumination variations corrections with feature based image processing in calibration process

- Depth-color relationship for improved bathymetric maps

- Previous approaches - Image Processing based
  - Reference histogram matching- Redistribute initial histogram bins to reshape into the shape of reference histogram
    - Why not - Difficult to determine the universal reference histrogram
  - Neighbouring histogram matching- Match each histogram to its neighbor histogram to smooth out local differences
    - Why not – Errors add up over on a larger scale

- Proposed approach – Physics based
  - Beer-Lambert Law – flow depth from brightness levels in imagery

$$I_{out} = I_{in} e^{-cx}$$

where c is rate of absorption of medium – depends on properties of medium such as turbidity and frequency of the incident light

3.2 Method 2 – Approach

- Identify wet/dry interface using image classification
  - Image classification – into dry and wetted areas
    - Accuracy of 80% of pixels being correctly classified automatically
    - Higher level of accuracy required – therefore semi automatic interface developed in MATLAB to allow for manual corrections by humans
- Use brightness levels of unsubmerged clasts as I_{in}
- Calibrate Rate of absorption (c) using I_{in} and I_{out}
  - Assumed to be constant for the whole data set
  - Red color sensitive to bed depth variations as single pixel values
  - Bed material color variations are addressed by using averaging windows of different sizes; optimal is 66 by 66 pixels

Conventional: $I_{red} = 109.5e^{-0.596H}$

→ Illumination-corrected: $I_{red} = 128e^{-0.387H}$

Method 3

Automated Identification of River Hydromorphological Features

Casado M R, Gonzalez R B, Kriechbaumer T, Veal A (2015)

Goal: Feature classification of high resolution RGB aerial imagery using Artificial Neural Networks (ANN)

- River hydromorphological features such as riffle, banks, grass, shadow, vegetation, trees etc.

- Previous Approach: All using computer vision based techniques
- Proposed approach: Using supervised learning
  - ANN Architecture: 3 layered Multilayer Perceptron ANN with non-linear activation functions

3.3 Method 3 – Approach

- Flight Planning
  - Selection of flight area, direction of flight, GSD, imagery overlap, take off and landing points
  - Computation of flight height, number of flights and location of waypoints

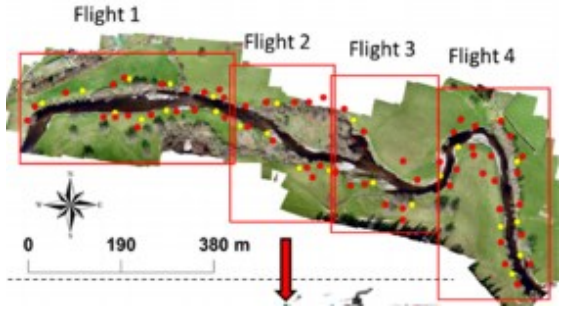

- Data Acquisition & photogrammerty
  - Distibution of Ground Control Points & Cross Points (with RTK GPS location information)
  - Visual identification of features
  - Selection of key images
  - Generation of segmatic products
  - Estimate photogrammetric accuracy

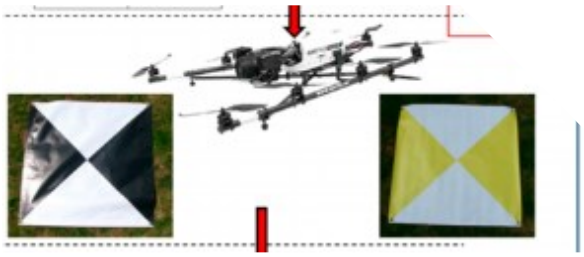

[Casado et al., 2015]

3.3 Method 3 – Approach

- Image Classification
  - Delineate the river channel
  - RGB image selection based on key feature presence
  - Conversion of the selected proportion from RGB to L*a*b
    - L (lightness), a (green to red scale), b (blue to yellow scale)
    - Helps to discriminate between green canopy cover from ground
  - Cluster analysis of the L*a*b output
  - Supervised selection of clusters
  - ANN Model training

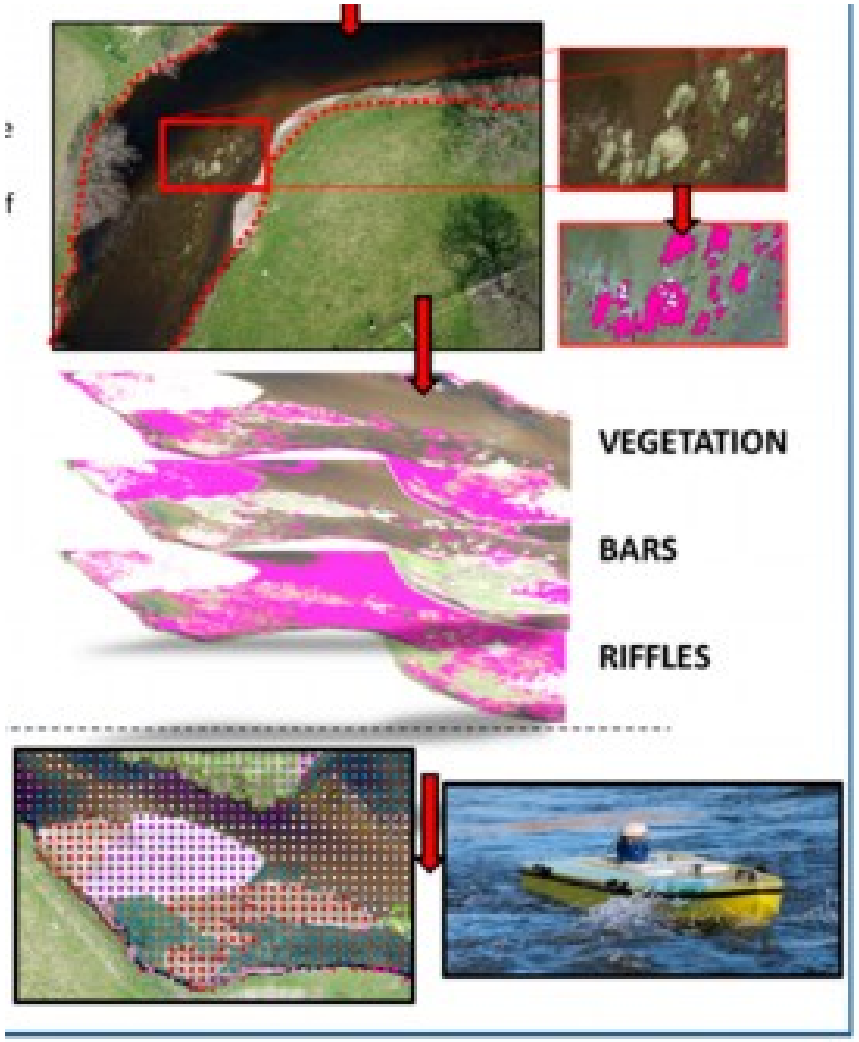

[Casado et al., 2015]

3.3 Method 3 – Approach

- Image Classification
  - Application of ANN to the orthorectified image
  - Quantification & Georeference of the area corresponding to each feature
- Validate results
  - Ground truth data - ADCP measurements
  - Visual classification

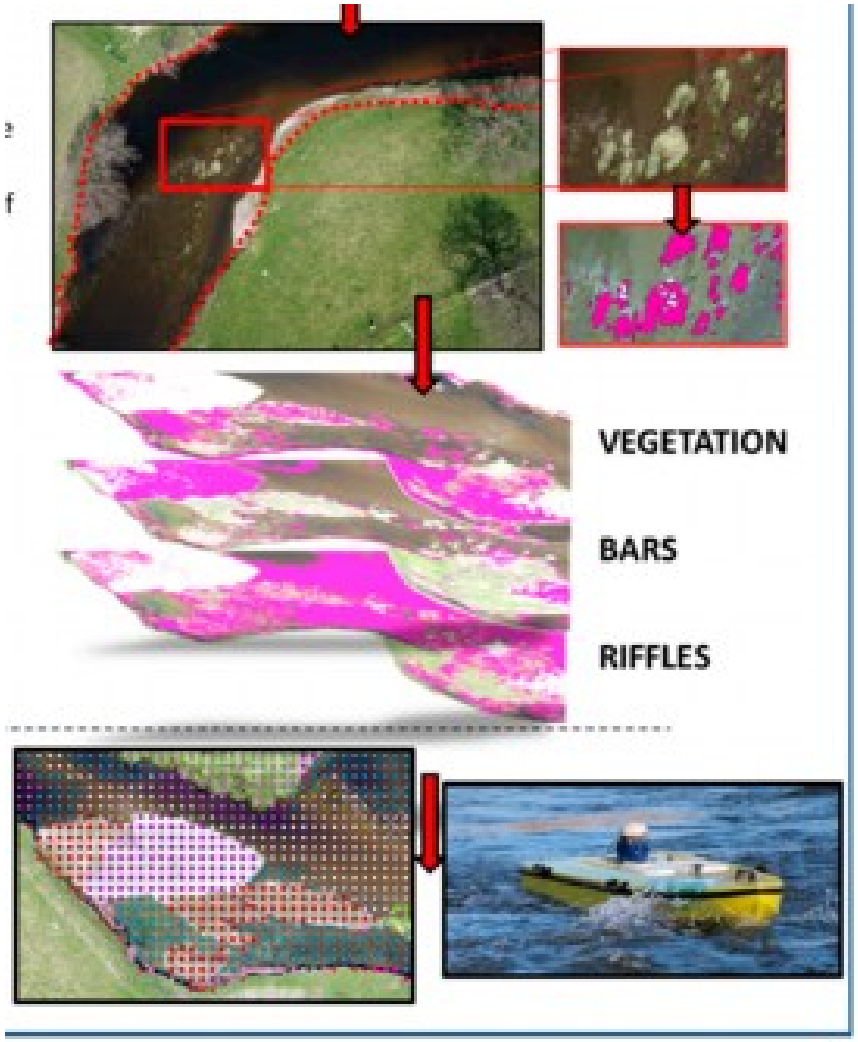

[Casado et al., 2015]

Data

4.1 Data - Method 1

- High resolution (3cm) aerial imagery (collected in August 2002)
- 80km of the Sainte-Marguerite River, Quebec, Canada
  - Dry: 19%, Shallow Water: 67%, Deep water: 14%
- Flying height – 155m, 60% overlap – 2092/4184 images used in study
- Field Data for Calibration and Validation
  - ~600 artificial targets placed along river for Georeferencing using ArcMap by ESRI
  - Manually sensed to prepare ground truth data
  - 39 georeferenced manual samples of the surface grain size in the wetted perimeter (estimated error: ±29.7cm)
    - For each site, 10 clasts and water depth measurements in the 1m squared area
  - Davey and Lapointe, unpublished report in 2004 is used as additional validation data – field based serdimentary links characterization by bulk sampling of the river bed material, inclusive of sand particles to boulder rapids

4.2 Data - Method 2

- High resolution aerial imagery (collected in August 2002)
- 80km of the Sainte-Marguerite River, Quebec, Canada
- 60% overlap – 2092/4184 images used in study
- Flying height – 155m, Ground resolution - 3cm
- Field Data for Calibration and Validation
  - 50 measurements (every 5m in 250m) to define the water surface elevation, beacuse no tributaries bring major input of sediment
  - 1500 GPS measurements for water depth– 1000 for calibration, 500 for validation
  - 250m study site covered in 4 images with 24 Grount Control Points

4.3 Data - Method 3

- High resolution aerial imagery (collected in April 2015)
- 1.4km of the River Dee, Wales, United Kingdom
- 60% along track & 80% cross track overlap – 394/746 images used
- Flying height – 100m, Resolution – 2.5cm
- Field Data for Calibration and Validation
  - 60 Grount Control Points (1m by 1m) distributed uniformly for external orientation with GPS (positioning accuracy of 1.2cm)
  - Additional 25 Yellow and white check points for image coregistration model errors
  - River velocity and depth measurements and their variability by Acoustic Doppler Current Profiler (ADCP) on a boat in a zig zag pattern
- Key to success of ANN: Adequate selection of small proportion of imagery used for training and calibration process.
  - The features were present for more than 50% of the selected area
  - Images with shadows or confusing features were not selected

Results & Discussion

- Median diameter as a function of local semivariance of region
  Only for dry areas: $D_{50} = 0.34SV + 10.12$ (Precision: ±11mm)
  Only for wet areas: $D_{50} = 1.33SV + 18.95$ (Precison: ±29mm)
  - 85% level of explanation in the wetted region relationship

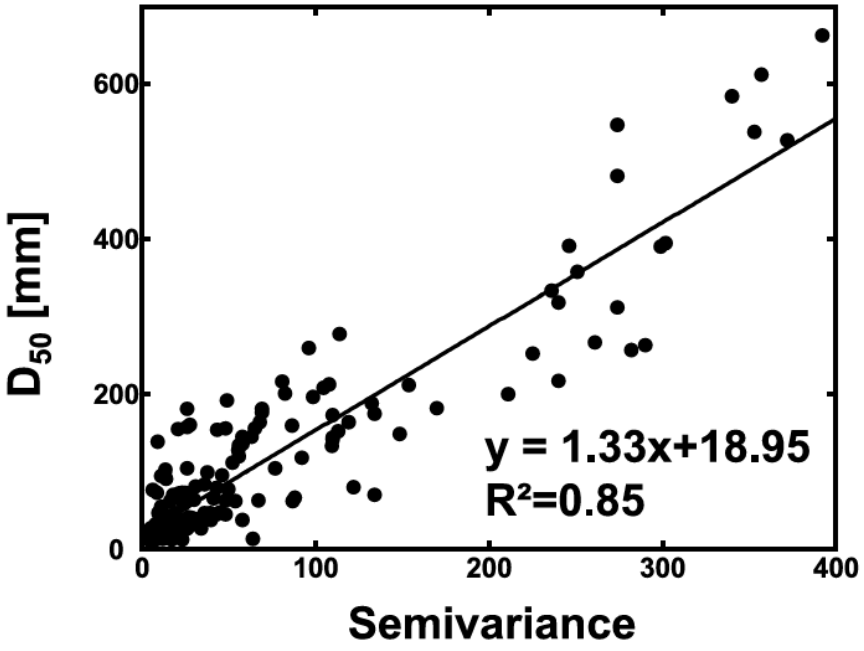

Calibration model for grain size estimation in submerged areas

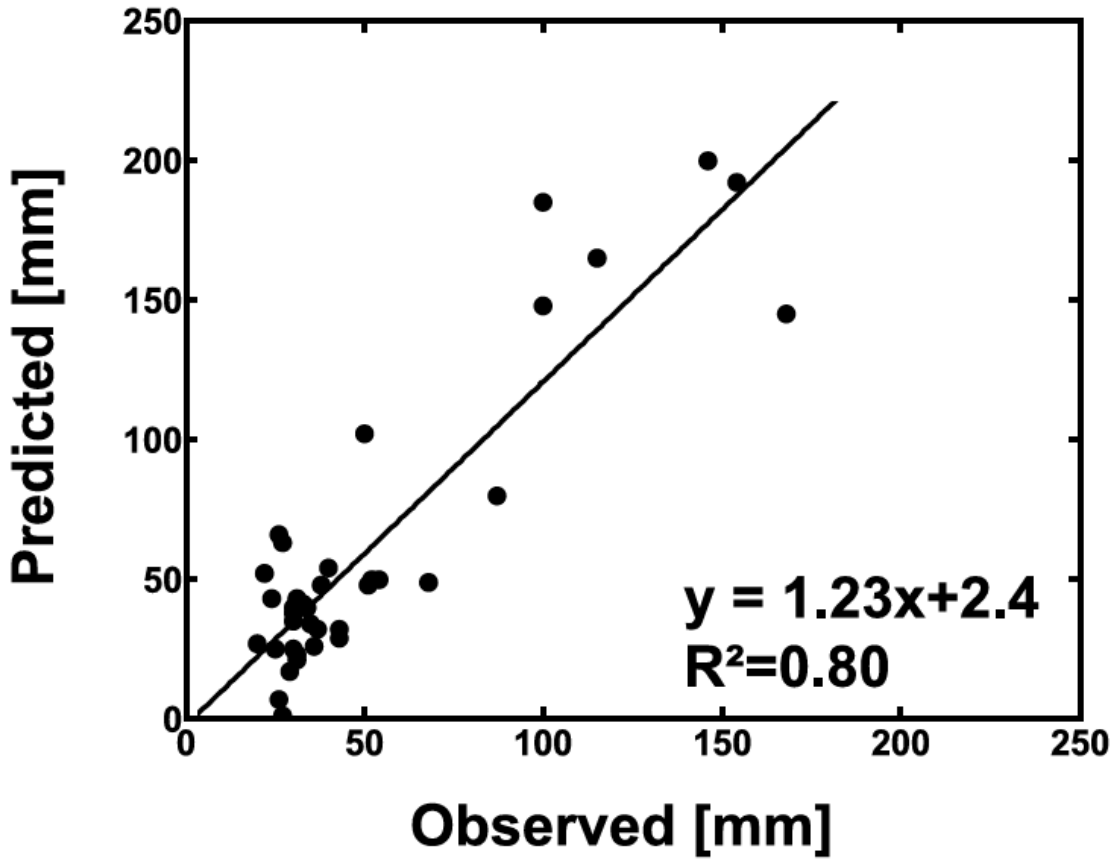

Validation results for grain size estimation in submerged areas

- Sources of error
  - Effect of water depth – poorer grain size estimates at deeper parts
    - For flows < 50cm from water surface: Accuracy (8mm), Precision (±13mm)
    - For flows > 50cm: Accuracy (10mm), Precision (±15mm)
  - Effect of particle size relative to the average window used in calibration
  - Effect of substrate composition
    - Different rock types
    - Presence of algae on rocks

5.2 Results & Discussion – Method 2(1)

Conventional: $I_{red} = 109.5e^{-0.596H}$

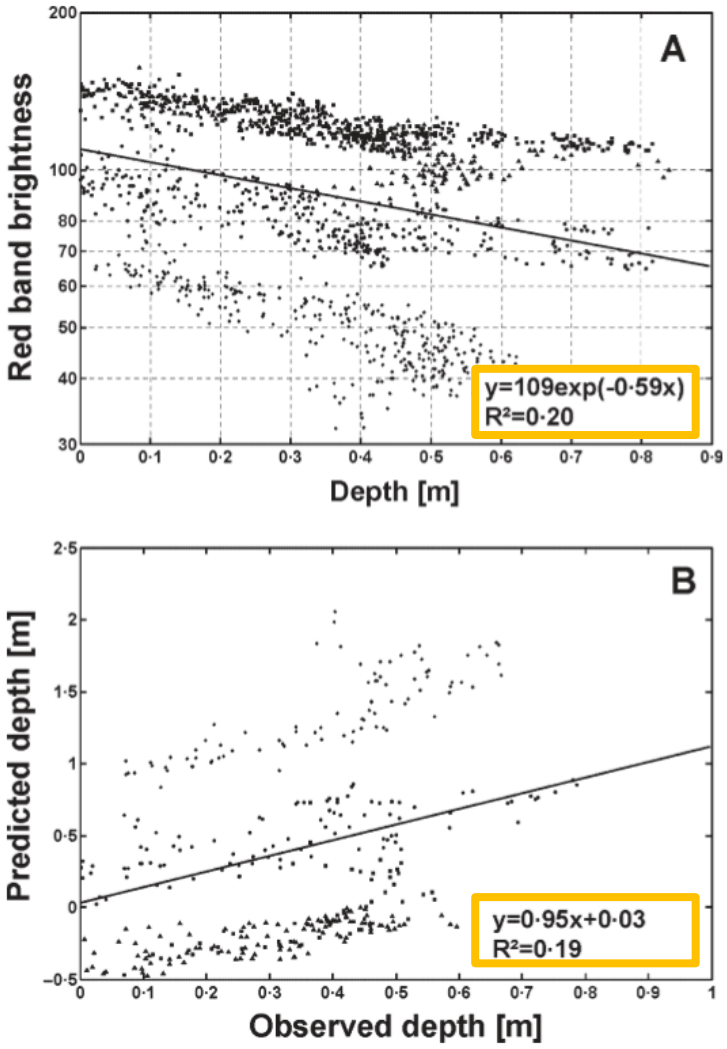

Illumination − corrected: $I_{red} = 128e^{-0.387H}$

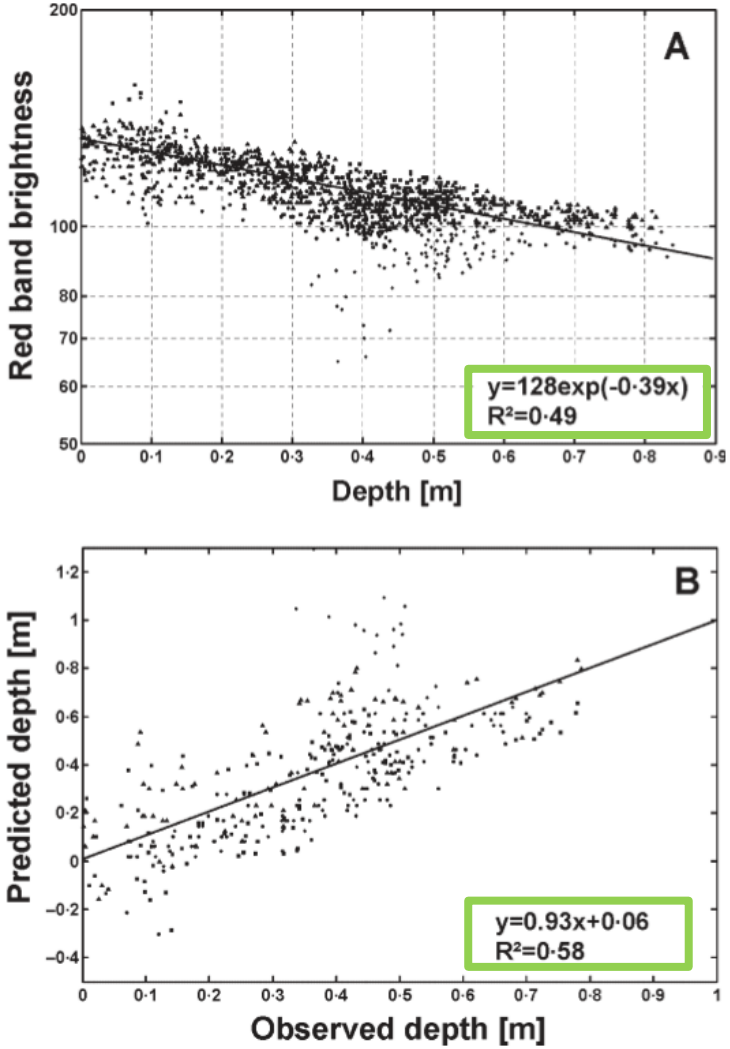

- Sources of error
  - Resolution differences in bathymetric map data (highly localized and spatial depth variability) and GPS validation data (cm precision)
  - Assumed constant rate of absorption (c), fails for white water rapids
  - Bank shading – falsely implies deeper regions

5.3 Results & Discussion – Method 3(1)

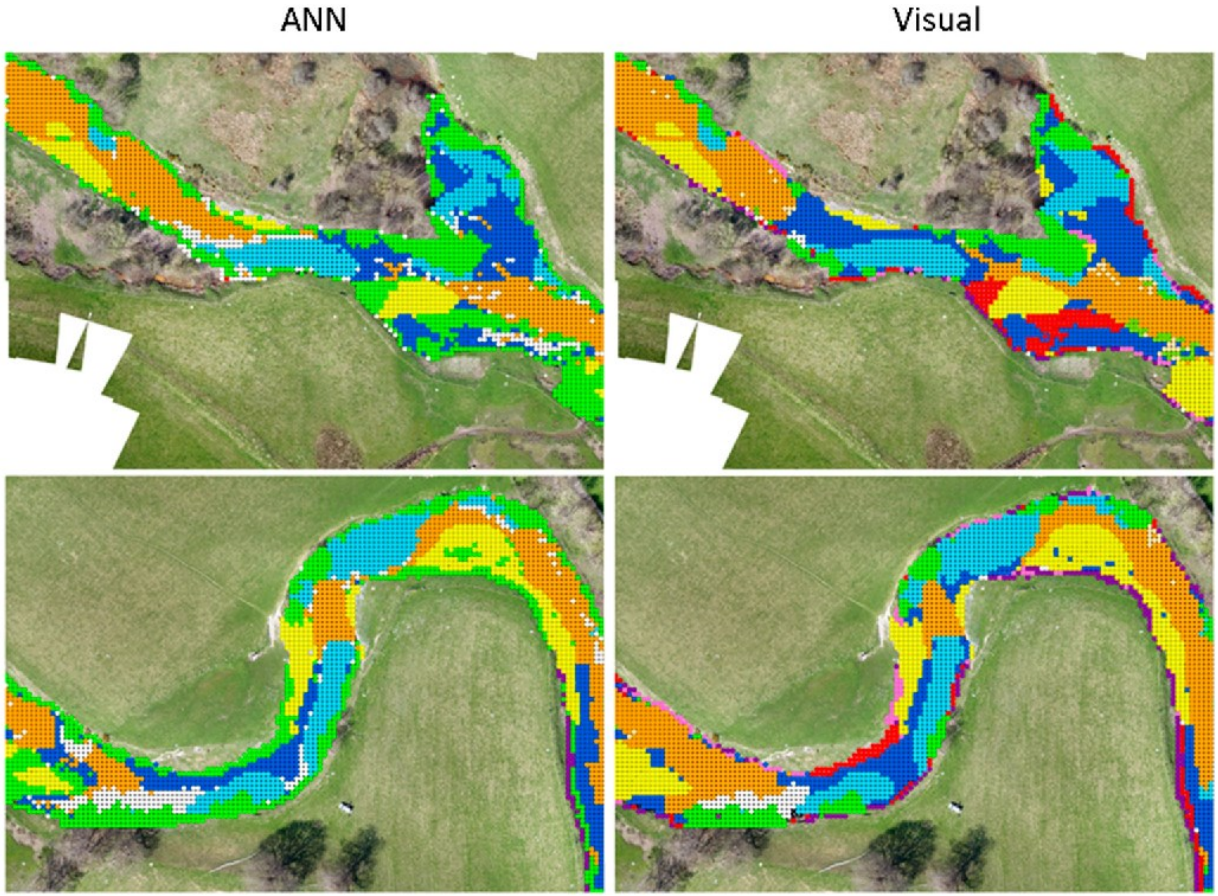

- 81% ANN Classification accuracy (10662/13085 points correctly classifed)
- True Positive Ratios > 85% for majority of classes
- ANN reached solution in less than 60 iterations

Table 3. Confusion matrix of visual classification (VC) *versus* Artificial Neural Network (ANN) classification. Feature codes have been abbreviated as follows: side bars (SB), erosion (ER), riffle (RI), deep water (DW), shallow water (SW), tree (TR), shadow (SH), vegetation (VG), vegetated bar (VB), vegetated bank (VK), submerged vegetation (SV), emergent vegetation (EV) and grass (GR). GE stands for georeferencing error.

	ANN Classification										
Feature	**VC**	**SB**	**ER**	**RI**	**DW**	**SW**	**TR**	**SH**	**VG**	**GE**	**Total**
SB	1334	1097	-	8	-	2	-	10	214	3	1334
ER	287	-	22	13	1	3	-	10	238	-	287
RI	3339	-	1	2717	-	318	-	219	76	8	3339
DW	2082	-	-	60	1927	54	-	8	29	4	2082
SW	2573	-	-	262	80	1514	-	493	217	7	2573
TR	1755	-	-	76	1	29	496	135	1013	5	1755
VB	299	-	-	-	-	-	-	-	299	-	299
VK	313	-	10	-	6	-	-	15	281	1	313
SV	468	-	-	160	-	125	-	46	135	2	468
EV	71	-	1	9	-	2	-	1	58	-	71
GR	344	-	-	-	-	-	-	-	343	1	344
SH	220	-	4	-	-	-	-	180	31	-	220
Total	13,085	1097	38	3305	2015	2052	496	1117	2934	31	13,085

Feature Identification (ANN)		TPR	TNR	FNR	FPR
Substrate Features	Bars	0.822	0.765	0.178	0.000
	Erosion	0.077	0.786	0.923	0.001
Water Features	Riffle	0.814	0.756	0.074	0.060
	Deep Water	0.926	0.741	0.074	0.008
	Shallow Water	0.588	0.815	0.412	0.051
Vegetation	Trees	0.860	0.757	0.140	0.082
	Vegetated Bar	1.000	0.765	0.000	0.082
	Vegetated Bank	0.898	0.767	0.102	0.082
	Submerged Vegetation	0.288	0.788	0.712	0.082
	Emergent Vegetation	0.817	0.770	0.183	0.082
	Grass	0.997	0.750	0.003	0.082
Shadow		0.818	0.770	0.182	0.073

Sources of error

- Georeferencing error ~ 0.2% of error in classification
- Erosion – eroded banks were vertical cliffs, limited 2D planar aerial view
- Shallow water – dark brown color due to shadow in areas with mossy submerged vegetation or sedimentation
- Vegetated banks – confused with erosion or shadows

5.4 Conclusion

Motivation	Method 1	Method 2	Method 3
River Characterization (Morphological fetaures)	Yes	Yes	Yes
River restoration & management (Algae & plant species)	No	No	Yes

- Datasets used – Generated by the authors based on area of interest
  - Method 1 and 2 – Same dataset
  - Method 3 – Different than above
- Datasets generated with well prepared flights - sufficient image overlap, validation points using Ground Control Points and GPS data for geo-referencing manual measurements

Comparison between three methods – Difficult!

Personal Opinion

6 Personal Opinion(1)

- Remote sensing plays an important role in getting valuable data for large water bodies remotely
  - Aerial imagery being the fine compromise between imagery resolution to fulfill the motivation and large scale analysis
  - Benefit - Solves the problem of river monitoring using aerial images with Physics-based Image Processing & ANN
  - Limitations
    - Limited by flying platform (eg. UAV) performance to collect data
    - Impractical to assume similar water flow properties along the entire river channel – therefore difficult in generating long river analysis using same methods
    - Not applicable for sand, silts and clays – too coarse for river scale feature analysis
  - Good datasets available, but only for specific rivers

- Future
  - Multiple sensor payloads on UAV without the weight factor compromising the flight time endurance
  - Multisensor integration and high-accuracy attitudinal information
  - Swarm technology for UAVs – Smarter surveying deployments - for scalable, efficient and robust, rapid acquisition of data – limited due to physical and legal constraints
  - Autonomous under water vehicle, Unmanned Surface Vehicle for bank morphology and vegetation
  - Real-time analysis and monitoring with combined datasets & Internet of Things such as prediction of flood events in real-time

Personal Opinion(3) - River Corridor Monitoring

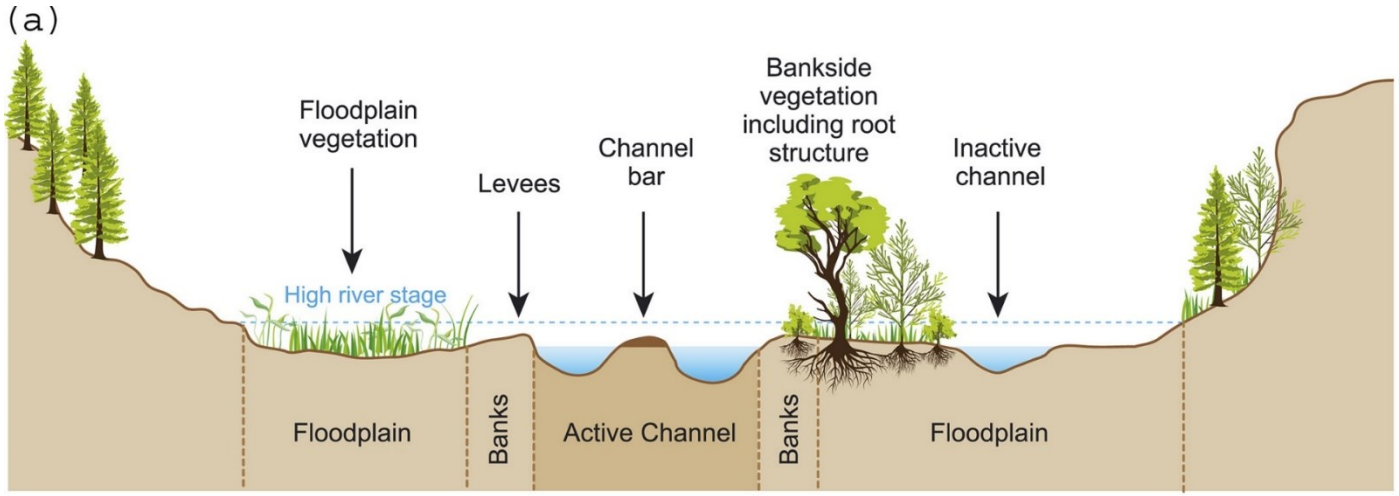

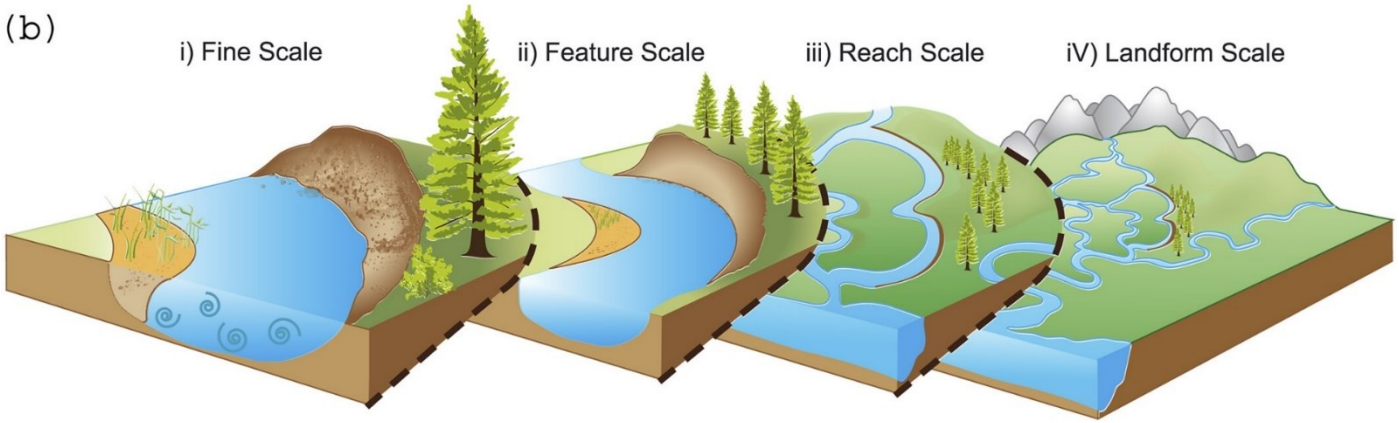

[Tomsett & Leyland (2019)]

Choosing a technique is site and parameter of interest dependent!

References (1)

- ArcGIS Pro: https://pro.arcgis.com/en/pro-app/help/analysis/geostatistical-analyst/understanding-a-semivariogram-the-range-sill-and-nugget.htm
- Bolognesi M, Farina G, Alvisi S, Franchini M, Pellegrinelli A, Russo P (2017). Measurement of surface velocity in open channels using a lightweight remotely piloted aircraft system. Geomatics Natural Hazards & Risk, 8(1), 73–86
- Brunier G, Fleury J, Anthony E, Pothin V, Vella C, Dussouillez P, Michaud E (2016). Structure-from-motion photogrammetry for high-resolution coastal and fluvial geomorphic surveys. Geomorphologie-Relief Processus. Environment, 22(2), 147–161
- Carbonneau P E, Lane S N, Bergeron N (2004). Catchment-scale mapping of surface grain size in gravel bed rivers using airborne digital imagery. Water Resources Research, 40(11)
- Carbonneau P E, Bergeron N, Lane S N (2005). Automated grain size measurements from airborne remote sensing for long profile measurements of fluvial grain sizes. Water Resources Research, 41(11), W11426
- Carbonneau P E, Lane S N, Bergeron N (2006). Feature based image processing methods applied to bathymetric measurements from airborne remote sensing in fluvial environments. Earth Surface Processes and Landforms: The Journal of the British Geomorphological Research Group, 31(11), 1413-1423

References (2)

- Casado M R, Gonzalez R B, Kriechbaumer T, Veal A (2015). Automated Identification of River Hydromorphological Features Using UAV High Resolution Aerial Imagery. *Sensors (Basel, Switzerland)*, *15*(11), 27969–27989

- Dilley M, Chen R, Deichmann U, Lerner-Lam A, Arnold M (2005).Natural disaster hotspots: A global risk analysis. Retrieved from Washington, World Bank
- Ezequiel C A F, Cua M, Libatique N C, Tangonan G L, Alampay R, Labuguen R T, Favila C M, Honrado J L E, Canos V, Devaney C, Loreto A B, Bacusmo J, Palma B (2014). UAV aerial imaging applications for post-disaster assessment, environmental management and infrastructure development. In 2014 International Conference on Unmanned Aircraft Systems (pp. 274-283). IEEE
- Kummu M, de Moel H, Ward P J, Varis O (2011). How close do we live to water? A global analysis of population distance to freshwater bodies. PloS one, 6(6), e20578–e20578
- Flener C, Vaaja M, Jaakkola A, Krooks A, Kaartinen H, Kukko A, Alho P (2013). Seamless mapping of river channels at high resolution using mobile LiDAR and UAV-photography. Remote Sensing, 5(12), 6382-6407
- Fonstad M A, Dietrich J T, Courville B C, Jensen J L, Carbonneau P E (2013). Topographic structure from motion: A new development in photogrammetric measurement. Earth Surface Processes and Landforms, 38(4), 421–430

References (3)

- GIS Geography: https://gisgeography.com/spatial-autocorrelation-moran-i-gis/
- Graham D J, Rice S P, Reid I (2005). A transferable method for the automated grain sizing of river gravels. Water Resources Research, 41(7)
- Larson M D, Milas A S, Vincent R K, Evans J E (2018). Multi-depth suspended sediment estimation using high-resolution remote-sensing UAV in Maumee River, Ohio. International Journal of Remote Sensing, 39(15-16), 5472–5489
- Lee C S, Hsiao F B (2012). Implementation of vision-based automatic guidance system on a fixed-wing unmanned aerial vehicle. Aeronautical Journal, 116(1183), 895–914
- Lega M, Kosmatka J, Ferrara C, Russo F, Napoli R M A, Persechino G (2012). Using advanced aerial platforms and infrared thermography to track environmental contamination. Environmental Forensics,13(4), 332-338
- Lejot J, Delacourt C, Piégay H, Fournier T, Trémélo M L, Allemand P (2007). Very high spatial resolution imagery for channel bathymetry and topography from an unmanned mapping controlled platform. Earth Surface Processes and Landforms, 32(11), 1705–1725
- Rapple B, Piegay H, Stella J C, Mercier D (2017). What drives riparian vegetation encroachment in braided river channels at patch to reach scales? Insights from annual airborne surveys (Drome River, SE France, 2005-2011). Ecohydrology, 10(8), 16

References (4)

- Rathinam S, Almeida P , Kim Z, Jackson S, Tinka A , Grossman W, Sengupta R (2007). Autonomous Searching and Tracking of a River using an UAV. IEEE American Control Conference. 2007. 359 – 364
- Tomsett C, Leyland J (2019). Remote sensing of river corridors: A review of current trends and future directions. *River Research and Applications* **2019**, *35*, 779–803
- Westoby M J, Brasington J, Glasser N F, Hambrey M J, Reynolds J M (2012). 'Structure-from-Motion' photogrammetry: A low-cost, effective tool for geoscience applications. Geomorphology, 179, 300–314